^{4}He and ^{3}He Particles from Au, Bi, and Th Nuclides Bombarded by 157-MeV Protons

H. DUBOST, M. LEFORT, J. PETER, AND X. TARRAGO
Institut Joliot-Curie de Physique Nucléaire, Faculté des Sciences de Paris-Orsay, Orsay, France
(Received 23 July 1964)

Energy distribution measurements have been carried out for ^{4}He and ^{3}He at different angles when Au, Bi, and Th targets are bombarded by 157-MeV protons. The telescope method was applied to solid-state detectors. The angular distribution has two components. The first, due to an isotropic process, is attributed to the evaporation mechanism. The second, preferentially in the forward direction, is taken as evidence for a knock-out mechanism. Prompt cascade nucleons are believed to be scattered by α clusters on the surface of the nucleus and to eject α particles. About 40 nucleons may be organized in α clusters in heavy nuclei.

I. INTRODUCTION

IN recent years several studies of (p,α) reactions at medium energies have been reported and several possible models of the disintegration process have been discussed, especially the *evaporation* from highly excited nuclides and the *knock-out mechanism* of quasifree α particles from the nuclear surface. Also, the radiochemical study of excitation functions for the production of residual nuclei from targets bombarded with 50- to 200-MeV protons has shown evidence for a rather high probability of ^{4}He emission even from heavy nuclides.[1-2] Calculations have been done in order to estimate both energy spectra and cross sections which could be expected from the evaporation process. The treatment was based on the statistical model of the nucleus and starts from the Weisskopf formalism.[3] Assuming the Fermi gas model for the nucleus, a stepwise Monte Carlo method was adopted by Dostrovsky *et al.*[4] These authors have studied systematically the effects of variations of parameter values on the evaporation process, and many of their results are related to the ^{4}He evaporation.

On the other hand, several authors have observed that a rather large forward-peaked ^{4}He emission occurred when nuclear emulsions were bombarded by protons in the energy range 50–600 MeV. Hodgson[5] and Perfilov *et al.*[6] have suggested a knock-out mechanism described as a quasifree collision between prompt cascade nucleons and α clusters on the nuclear surface. Experiments on $(\alpha,2\alpha)$ reactions at 910 MeV by Igo *et al.*[7] have confirmed the idea that one could observe such α clusters since the maximum of quasielastic events was at the kinematic separation angle $\theta_1+\theta_2=87.5°$, which corresponds to that for two-body collisions. Further, the energies of the individual α particles at θ_1 and θ_2 correspond to the free two-body kinematical values. Although there are a number of studies on the α clustering for light nuclei like ^{6}Li, ^{9}Be, or 12C in which quasielastic p-α collisions can be observed without too many difficulties by angular correlation,[8] the evidence for it does not appear so nicely for heavy nuclides.

We tried, some time ago, to collect information by the study of secondary reactions[9] induced on the target by the α particles, and our conclusions seemed to support the knock-out mechanism. In order to explain the forward ^{4}He emission from Bi nuclides, we had to assume the presence in the nucleus of some 15 preexisting α clusters, which could be scattered by prompt cascade nucleons.[10] A mean kinetic energy of 10 MeV had to be assumed for these clusters inside the nucleus, in order to obtain a good fit between the experimental energy distribution and the calculation.

However, several approximations were made in establishing the integrated energy spectrum, and the thick-target method which was used gave only a rough idea of the angular distribution, i.e., forward to backward ratio.

Therefore, we have carried on counter experiments which gave us differential energy distributions and a precise angular distribution. At the same time the discrimination could be made between ^{3}He, ^{4}He, and other emitted particles.

II. EXPERIMENTAL EQUIPMENT

1. Detectors

A ΔE, E counter telescope was used for particle detection. We used several ΔE counters in order to explore the energy distribution with the best accuracy, especially in the threshold region. These were boron and phosphorus diffused junctions of area 64 mm^2. A 100-μ thickness was adopted for the selection of 14- to 30-MeV ^{4}He and a 200-μ thickness was used for 22- to 80-MeV particles. The E detector was a lithium-drifted thick

[1] M. Lindner and A. Turkevich, Phys. Rev. **119**, 1632 (1960).
[2] M. Lefort, G. Simonoff, and X. Tarrago, Nucl. Phys. **25**, 216 (1961).
[3] J. M. Blatt and V. F. Weisskopf, *Theoretical Nuclear Physics* (J. Wiley & Sons Inc., New York, 1952).
[4] I. Dostrovsky, Z. Fraenkel, and G. Friedlander, Phys. Rev. **116**, 683 (1959).
[5] P. E. Hodgson, Nucl. Phys. 8, 1 (1958).
[6] V. I. Ostroumov, N. A. Perfilov, and R. A. Filov, Zh. Eksperim. i Teor Fiz. **39**, 105 (1960) [English transl.: Soviet Phys.—JETP **12**, 77 (1961)].
[7] G. Igo, L. F. Hansen, and T. J. Gooding, Phys. Rev. **131**, 337 (1963).
[8] C. Ruhla, M. Riou, M. Gusakow, J. C. Jacmart, M. Liu, and L. Valentin, Phys. Letters **6**, 282 (1963).
[9] H. Gauvin, M. Lefort, and X. Tarrago, Nucl. Phys. **39**, 447 (1962).
[10] H. Gauvin, M. Lefort, and X. Tarrago, J. Phys. **24**, 665 (1963).

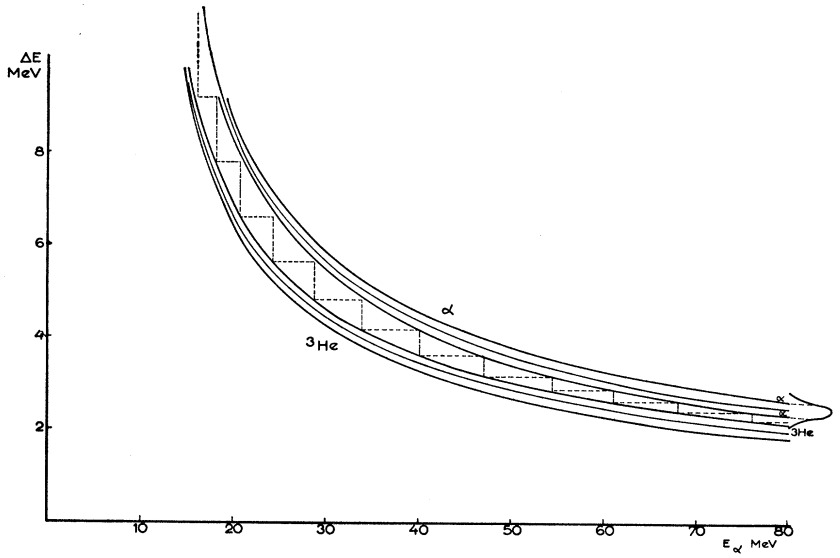

FIG. 1. dE/dx versus E relationships for ^{4}He and ^{3}He. Curves on both sides of the main line represent the limits for the half-width of the straggling effects in the dE/dx.

junction with a resolution of 40 keV. The total resolution was of the order of 100 keV, which is good enough since the energy-loss fluctuation (half-width of the distribution) in such a ΔE detector is of the order of 300 to 400 keV for α particles which leave between 2 and 10 MeV along their paths. The experiments were performed in a one-m scattering chamber and the distance between the target and the E detector was 30 cm. The determination of the solid angle was done both by geometrical calculations and by putting at the target position an active deposit from thorium emanation. The α emission rate of this deposit was first calibrated with a 2π ionization chamber, and the 8.78-MeV α rays were then counted again with the E detector in the scattering chamber. The solid angle was found to be $4\pi/26\,730$ sr.

2. Targets and Beam Calibration

Gold and thorium targets consisted of rectangular laminated thin foils 5×10 cm. Their thicknesses were respectively 16.8 and 37.5 mg/cm. The bismuth target was prepared by evaporation of the metal under vacuum and condensation on a Mylar film. The thickness was accurately measured by several methods and found to be 13.2 mg/cm.

The target was put in the plane perpendicular to the direction of the telescope for the angles 20°, 45°, 135° and 160°. For angles near 90°, the target was left at 45° to the beam. We checked that the entire beam section was always seen by the telescope.

The number of protons through the target was measured on an ionization chamber, which had been calibrated with a Faraday cup. The beam is extracted from the Orsay 157-MeV synchrocyclotron by means of an auxiliary frequency,[11] and the intensity was of the order of 10^9 protons per second.

[11] A. Cabrespine, J. Phys. **21**, 332 (1960).

3. Electronics and Energy Calibration

We have drawn curves for dE/dx values against E for ^{4}He and ^{3}He, from the tables of Williamson and Boujot.[12] Each energy-loss value in the tables represents a mean, since there is a more or less Gaussian distribution of the energy loss around a mean value for a given energy and a given thickness.[13] We have drawn, on both sides of the curve, two curves which correspond to the half-widths of these distributions (Fig. 1).

A block diagram of the electronics is shown in Fig. 2. The preamplifiers are put next to the junctions inside the reaction chamber. Pulses from both detectors are put in coincidence $2\tau=6\times10^{-8}$ sec. Pulses from the rapid coincidence circuit are sent to a triple coincidence slow circuit ($2\tau=5\times10^{-7}$ sec). The ΔE pulse is amplified and put into two selectors. The ΔE bands were chosen in such a way that the discrimination between ^{3}He and ^{4}He would always be unambiguous. The output from the selectors enters into the slow coincidence circuit.

A sum circuit adds the two pulses from ΔE and E in order to obtain the information on the total energy.

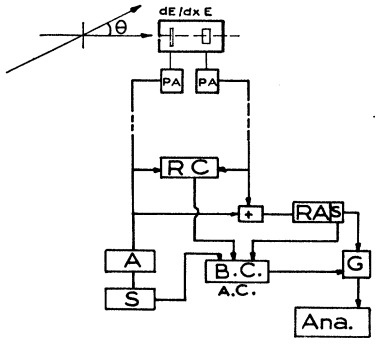

FIG. 2. Electronics block diagram.

[12] C. Williamson and J. P. Boujot, Table of Ranges and Rates of Energy Loss of Charged Particles of Energy 0.5 to 150 MeV, Commissariat Energie Atomique: Report 2189, 1962 (unpublished).
[13] T. E. Cranshaw, Progr. Nucl. Phys. **2**, 271 (1952).

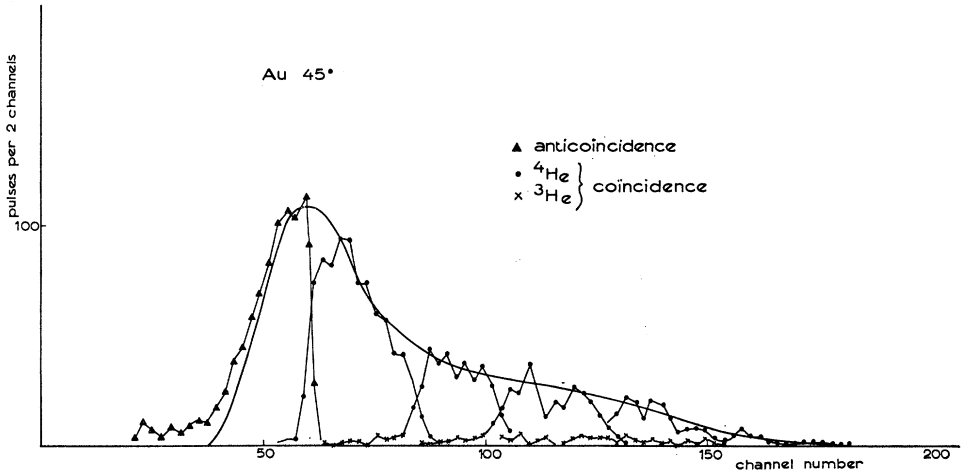

FIG. 3. Experimental energy distribution on gold target. α and ^{3}He counting rates were measured for selected energy intervals.

After amplification the pulse enters into the slow coincidence. The linear analysis of the total energy pulse is made by a 256-channel analyzer when the pulse has gone through a gate opened by the slow coincidence signal.

For the low part of the energy distribution (8–14 MeV), α particles are entirely stopped in the ΔE counter. We have used it as the E detector and put the rapid coincidence signal in anticoincidence on the slow circuit, in order to avoid any information from particles which would have gone through ΔE and E junctions.

The energy calibration of the counters was done in two steps. First the ΔE detector was calibrated with α particles from ^{210}Po (5.3 MeV) and from thoron deposit (6.09 and 8.78 MeV). Since such a calibration would cover only a very narrow region in the E counter (up to 80 MeV), we have used also the α particles during the experiment itself. When a narrow width is selected for ΔE by adjusting the selectors, the corresponding energy is well defined. We have found that the E detector response was entirely linear through all the energy range from 6 to 80 MeV.

III. EXPERIMENTAL RESULTS

1. Energy Distributions for ^{4}He and ^{3}He

Values for $d^2\sigma/dEd\Omega$ have been measured for the three targets (Au, Bi, Th) and for laboratory angles of 20°, 45°, 65°, 90°, 105°, 135°, and 160°. A typical set of experimental points is given in Fig. 3. We have measured the same spectra with several detectors, and all the results are consistent.

Since the targets were not very thin, it was necessary to make corrections to the experimental results for the effects of energy degradation. We have considered the target as a stack of I very thin foils. An α particle detected with the energy E_j can be formed from any of the I foils. Its original energy was $E_i=E_j+\Delta E_i$, if ΔE_i is the energy lost through i stacked foils. To a measured energy E_j, there correspond several original energies E_i with $E_j<E_i<(E_j+\Delta E)$, if ΔE is the energy loss through the total thickness. We have calculated the corrected energy spectra by use of a CAB 500 electronic computer. The main effect of the corrections is a shift of the spectrum toward higher energies. At the low-energy end the shift is 2 MeV and at the upper energy end it is half a MeV. Differential energy spectra are presented in Fig. 4.

2. Angular Distributions

For the three targets the energy-integrated angular distributions are presented in Fig. 5. The shapes of the curves show that two components are responsible for the cross sections. Since $d\sigma/d\Omega$ values are nearly the same[14] at 160° and 135°, we can estimate the isotropic contribution in the center-of-mass system.

We have made the assumption that this contribution is due to an evaporation process and we have tried to estimate what angular distribution should be observed in the laboratory. However, there is not a unique excitation energy since direct cascades occur between incident protons and the nucleons. For heavy nuclides, the isotropic distribution is modified by 6% with an excitation energy of 165 MeV (compound nucleus) and by less than 4.5% with an excitation energy of 90 MeV, which is the average value obtained in Metropolis calculations. When the correction has been made, it is possible to estimate the second component, which is peaked in the forward direction, mainly between $\theta=90°$ and $\theta=0°$, although there are some particles emitted at 105°.

Going back to the differential cross sections $d^2\sigma/d\Omega dE$, the energy distributions for the nonisotropic process are plotted in Fig. 4. We have drawn also differential angular distributions by plotting $d^2\sigma/d\Omega dE$ against angle at several different α-particle energies (Fig. 6). This shows that the most energetic particles are emitted at the smallest angles.

[14] The transformation from the laboratory system to the center-of-mass system affects the $d\sigma/d\Omega$ values at these two angles by less than 1%.

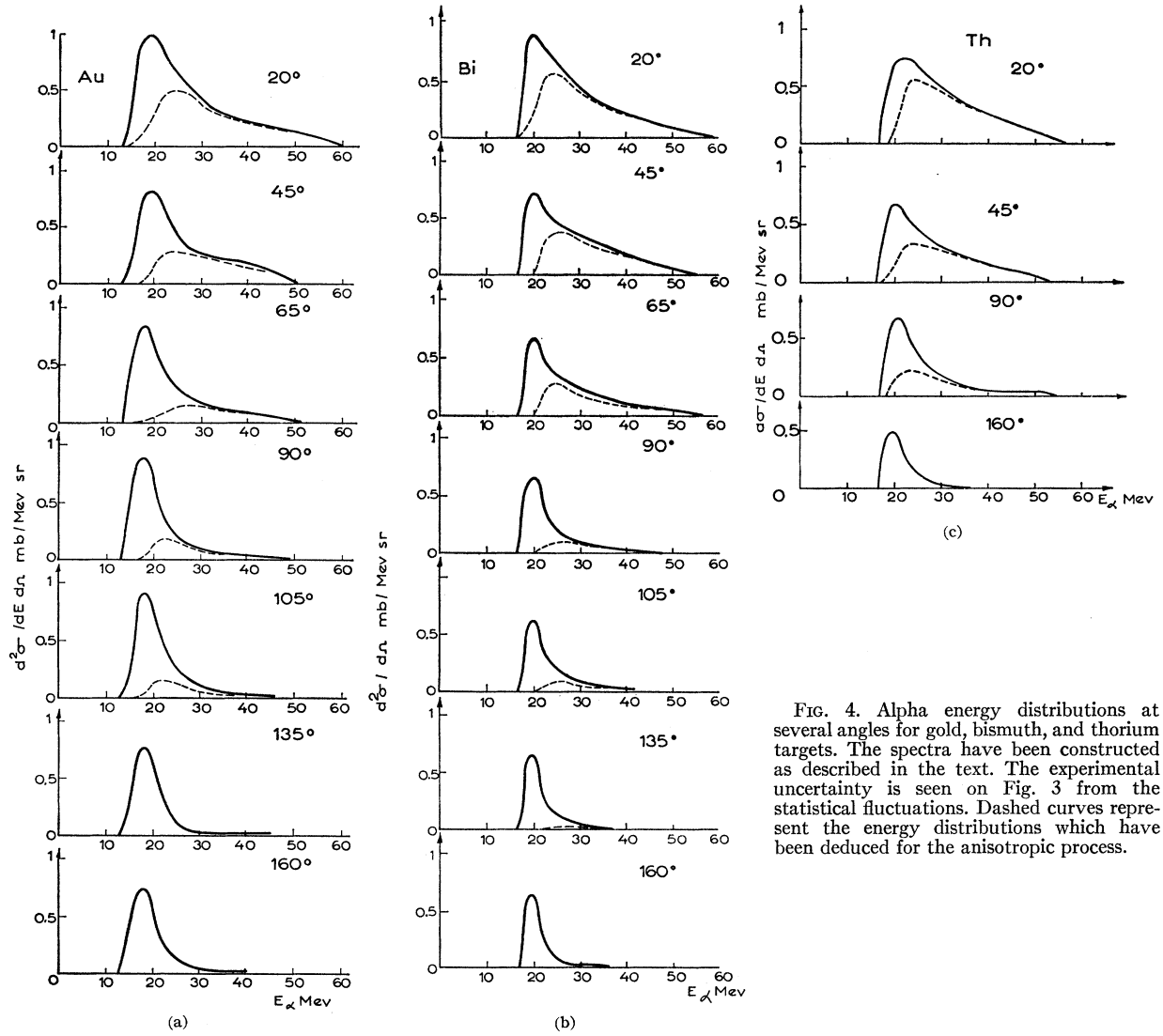

FIG. 4. Alpha energy distributions at several angles for gold, bismuth, and thorium targets. The spectra have been constructed as described in the text. The experimental uncertainty is seen on Fig. 3 from the statistical fluctuations. Dashed curves represent the energy distributions which have been deduced for the anisotropic process.

3. Integrated Energy Spectrum and Total Cross Section for α Particles

In order to make a comparison with radiochemical results and to obtain useful data for further calculations, the nonisotropic energy distribution integrated over all angles, $d\sigma/dE = 2\pi \int_{\theta=0}^{\theta=105°} (d^2\sigma/dE d\Omega) \sin\theta d\theta$ has been calculated for the three targets (Fig. 7).

In Table I we give total cross sections, evaporation cross sections (isotropic in the center-of-mass system) and nonisotropic process cross sections, which we call "direct interaction."

TABLE I. Cross-section values for production of α particles from Au, Bi, and Th irradiated by 157-MeV protons.

Target	σ total (mb)	σ evaporation	σ direct interaction
Au	109±15	72±10	37±8
Bi	82±10	45±7	37±7
Th	81±10	37±5	44±10

4. Energy Distribution and Cross Sections for Helium-3 Particles

Total cross sections for helium-3 are much smaller. They have been estimated to be 7±2 mb for gold and bismuth targets, and the statistics are too poor to yield a very good energy distribution at each angle. However, we have drawn on Fig. 8 an integrated energy spectrum $2\pi \int (d^2\sigma/dE d\Omega) \sin\theta d\theta$.

IV. REMARKS OF THE ^{4}He EMISSION

We shall discuss separately three main results from these experiments.

1. Evaporation Cross Sections

The cross-section values in Table I for the three targets are much larger than the cross sections which were deduced from the study of secondary reactions.[9] The reason is obvious when one considers the energy distribution. The α particles which can induce secondary

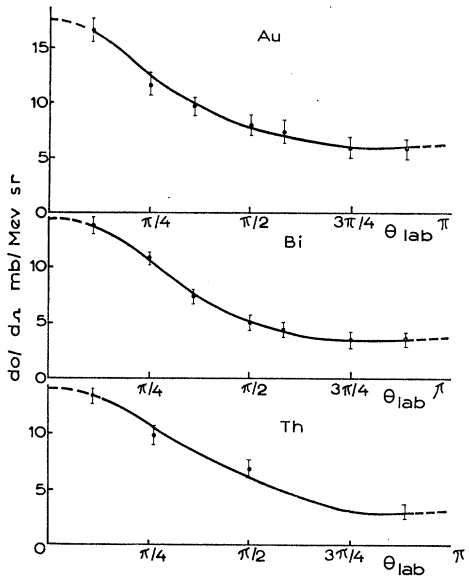

FIG. 5. Angular distributions in the laboratory for Au, Bi, and Th.

$(\alpha,2n)$ reactions in bismuth must have energies of at least 22 MeV, but more than $\frac{3}{4}$ of the evaporation distribution occurs at lower energies. Our preliminary results with counters[15] also yielded lower values because of the presence of a dead layer on the E counter which did not allow the detection in it of α particles with energies lower than 21 MeV.

When we compare our evaporation cross sections with data obtained by Muto *et al.*[16] at a lower energy (56 MeV), there is a reasonable increase, as shown on Fig. 9. Also it seems that the agreement is good with the estimations made for 240, 420, and 550 MeV, although these were made by the secondary reactions method. It should be noticed that the evaporation energy

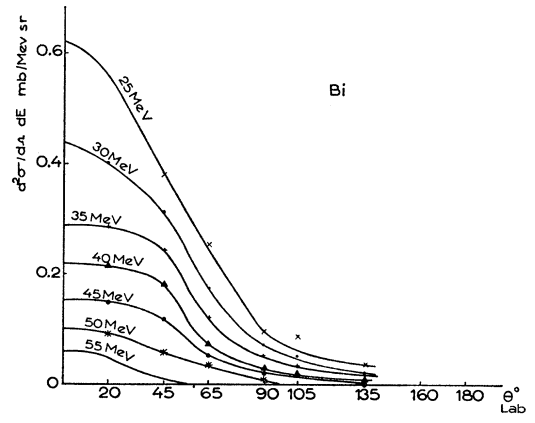

FIG. 6. Differential angular distributions for α particles of several energies for Bi targets.

[15] H. Dubost, M. Lefort, J. Peter, and X. Tarrago, Phys. Letters **9**, 146 (1964).

[16] J. Muto, H. Itoh, K. Okamo, N. Shiomi, K. Fukuda, Y. Omori, and M. Kihara, Nucl. Phys. **47**, 19 (1963).

distribution is shifted to higher energies when the excitation energy increases and therefore the experimental threshold of 22 MeV does not involve such a drastic elimination of α particles. The comparison with calculated values[4] depends on the choice of r_0, of the effective Coulomb barrier, and of the parameter values in the level density formula.

Da Silveira,[17] in our laboratory, has carried out Monte Carlo calculations and made a systematic study of the influence of these parameters for incident energies of 56 and 157 MeV, which correspond to the work of Muto *et al.* and to our work. Agreement can be obtained only when everything possible is done in order to decrease the calculated cross sections, i.e., $r_0=1.3$ F, level-density parameter $a=A/10$, pairing effect, low proportions of compound nucleus in the first step interaction. On the other hand, we shall see that the

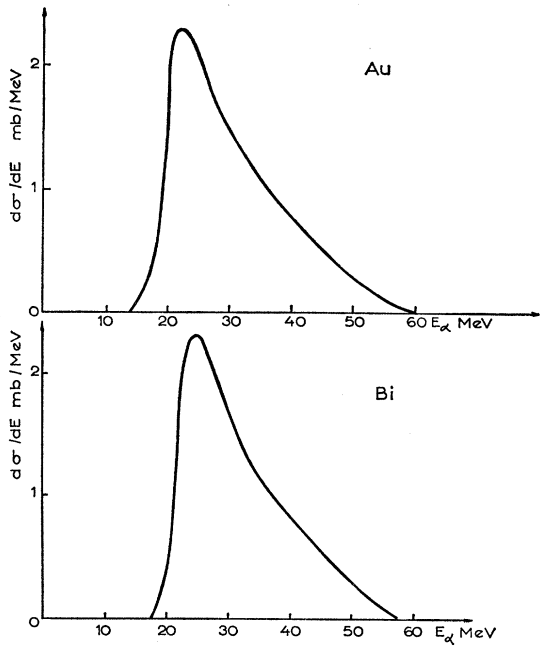

FIG. 7. Integral energy spectra for the anisotropic process in Au and Bi.

threshold of the energy distribution is very low; and it seems to be difficult to use a small r_0 value and a high Coulomb barrier in order to fit the cross section and at the same time explain the low-energy part of the α emission. We shall come back to this point later.

The last remark on the cross-section values relates to the comparison among gold, bismuth, and thorium. The rather small decrease (45 ± 7 to 37 ± 5) between bismuth and thorium, even if it is significant, can be accounted for by the Coulomb barrier variation (Z increases from 83 to 90). In contrast, this Coulomb barrier effect is not sufficient to explain the change (72 to 45) from Au to Bi, which seems beyond experi-

[17] R. Da Silveira, thesis, Paris, 1964 (unpublished).

mental errors. We believe that some additional contribution is due to a closed-shell effect when the target is changed from Au to Bi.

2. Energy Spectra for the Evaporation Process

Energy distributions have the usual shapes of evaporation spectra (for example in Fig. 4 at large angles 160°), but we have been surprised to find low-energy values at threshold and at maximum cross section for the three targets. Although the effective barrier can be estimated at some 20 MeV for Bi, even with a large value of r_0 (1.4 F), our experimental results show a threshold at 13±0.5 MeV for gold and 16.4±1.0 MeV for Bi, and cross section maxima at 20 MeV. These data are slightly higher than the results of Muto *et al.*[16] but it should be noticed that the average excitation energies are higher for 157-MeV protons than for 56-MeV protons. Da Silveira will discuss this question in more detail elsewhere. His conclusion is that it might be possible to reconcile low cross sections and low threshold if one makes a more refined estimation of the inverse-process cross section in the calculation of the probability of evaporation, and if one keeps a low r_0 value (1.25 or 1.3 F). There is also the possibility of deformation for excited nuclei, which yields low-energy charged particles in the direction of large deformation.[18]

3. Direct Interaction Process for the Emission of α Particles

We have confirmed the main conclusion of our previous work with secondary reactions. There is an important contribution of α particles emitted in the forward direction which cannot be attributed to the evaporation process. Its amount is about the same for the three heavy targets (40 mb±10). (The estimate from secondaries was 60±10 mb.) In Fig. 4, it can be seen that thresholds for this process are about 4 MeV higher than the evaporation threshold and in good agreement with the calculated Coulomb barrier. This

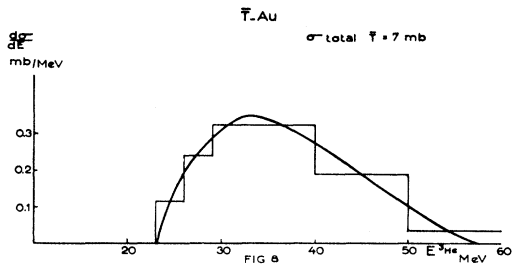

FIG. 8. Integral energy distribution for ^{3}He in gold.

[18] R. Da Silveira, Phys. Letters **9**, 252 (1964).

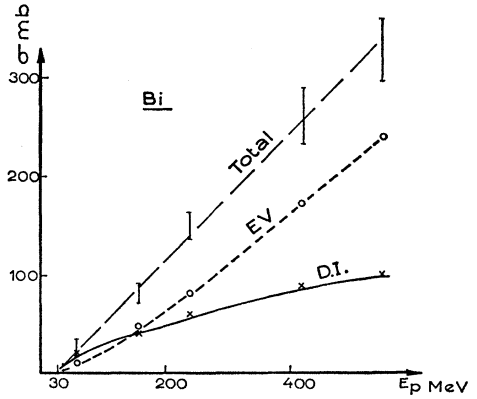

FIG. 9. Estimated excitation function for the α emission from bismuth. Cross sections are given for the evaporation process and for the direct interaction (D.I.). The data at 56 MeV are from Ref. 16 and the data at 240, 420, and 550 MeV are from M. Lefort and X. Tarrago, Nucl. Phys. **46**, 161 (1963).

observation supports the description of the second group of α particles as being produced by a knock-out process, as distinct from an evaporation mechanism; in evaporation, particles are observed for below the barrier because of high nuclear-level densities associated with low-energy loss in the evaporated particles.

The general shape of the spectrum is similar to that obtained with the secondary reactions, except for the low-energy part, which, as has been mentioned, extends to lower energies in the counter experiments. Therefore we believe that this new set of data gives some additional support to the *knock-out hypothesis*. An effort was made,[10] with a very approximate type of calculation, to fit the second component of α particles with the knock-out model. The result of this attempt was to show that a detailed calculation of a Monte Carlo type would be required for a meaningful comparison. If a diffuse-edge model is taken to describe the nucleus, one could include alpha clusters in the edge where nuclear matter is not so dense, and treat the kinematics in that part of the nucleus, taking account of (p-α) and (n-α) collisions. Our results can only suggest that in such a treatment one could guess that between 5 and 10 α clusters should be included with an average kinetic energy of $W \approx 10$ MeV.

ACKNOWLEDGMENTS

The authors wish to thank M. Corbet, E. Festa, and A. Richard, who built the electronics equipment. We are grateful to A. Coche and P. Siffert, from the Strasbourg Nuclear Chemistry Research Center, who made the solid state detectors used in this work. We are indebted to Maurice Perlmann for valuable discussions of this work and for many corrections in the English text.